Investigating neurochemical techniques for assessment of nerve regenerates within polymer guides

Chung-Chia Chen[1,2], Chu-Ying Chan[2], Li-Shu Chen[2],

Fuu-Jen Tsai[2], Chun-Hsu Yao[2,3†],Chin-Chuan Tsai[4,5†], Yueh-Sheng Chen[2,3*†]

[1]*Department of Chinese Medicine, Taipei City Hospital, Taipei, Taiwan*
[2]*Lab of Biomaterials, School of Chinese Medicine, China Medical University, Taichung, Taiwan*
[3]*Department of Biomedical Imaging and Radiological Science, China Medical University, Taichung, Taiwan*
[4]*School of Chinese Medicine for Post-Baccalaureate, I-Shou University, Kaohsiung, Taiwan*
[5]*Chinese Medicine Department, E-DA Hospital, Kaohsiung, Taiwan*

Running title: Neurochemical assessment of regenerated nerves

†These authors contributed equally to this work.

*Corresponding author: Yueh-Sheng Chen, PhD

Lab of Biomaterials, School of Chinese Medicine,

China Medical University, Taichung, Taiwan

Tel.: 886-4-22053366 ext. 3308; Fax: 886-4-22032295

E-mail: yuehsc@mail.cmu.edu.tw

Abstract

This research evaluated the use of proteins associated with neurite outgrowth, synapse formation, and Schwann cell proliferation as surrogate measures for peripheral nerve regeneration. Rat sciatic nerve regeneration was across a 10-mm gap in silicone rubber conduits (SRCs), genipin-crosslinked gelatin conduits (GGCs), and porous GGCs (PGGCs). After 8 weeks, axonal growth of regenerated nerves was determined using light microscopy and computer-based quantitative image analysis. Expression of the axonal growth associated protein 43 (GAP-43), the synaptic protein synapsin I, and the transforming growth factors type β (TGF-βs) in regenerated nerves were assessed simultaneously by Western blot. As a result, the nerve regenerates in the silicone rubber conduits had a relatively larger area containing more myelinated axons compared to those in the PGGCs and the GGCs. The levels of GAP-43 and synapsin I, but not TGF-β, correlated well with axonal growth in the regenerated nerves. These data suggest that SRCs could provide a more stable and suitable growth environment for regenerating axons than PGGCs and GGCs. In addition, GAP-43 and synapsin I may be a useful indicator of the status of regenerating axons in bridging conduits with different construction and physical properties.

Keywords: Nerve injury, Nerve repair, Nerve regeneration

1. Introduction

Tissue engineering has grown as an interdisciplinary field combination of cells, engineering and biomaterials [1]. Specific biochemical functions were performed using cells within an artificially-created support system to improve or replace biological tissues, such as heart [2], skin [3], and bone tissues [4]. Recently, the use of *in vitro* systems to assess developmental neurology is gaining momentum, and a number of neuronal models have been used for examining potential biomaterials for nerve regeneration. In particular, phenochromocytoma and Schwann cells have been widely used to screen biocompatible materials as a model of neuronal proliferation and differentiation [5-8]. However, there are limitations to the use of these cell lines. First, they do not develop true axons, dendrites, or synapses with each other. In addition, genetic drift with respect to repeated cell passage with a concomitant change in phenotype could happen [9]. Therefore, *in vivo* models are necessary to be used for revealing the real regeneration process in the developing nervous system.

Nerve bridge conduits have been used to study nerve regeneration *in vivo* [10-12]. The nerve bridge technique is the introduction of both ends of the injured nerve stumps into a tubular chamber, which can aid guidance of growing nerve fibers along appropriate paths and can enhance the precision of stump approximation. Several synthetic materials, either nondegradable or biodegradable, have been used as a nerve

conduit. In the nondegradable materials, silicone rubber is the most acceptable material applied to construct the nerve guide, mainly for its stable properties. It has been demonstrated that silicone rubber conduits (SRCs) are well tolerated in humans even after 3 years of implantation [13]. Numerous biodegradable materials have been used to construct nerve guides to repair injured nerves, such as poly-lactic acid and poly-glycolic acid [14,15]. Recently, a biodegradable material composed of genipin-crosslinked gelatin has also been used to make nerve regeneration chambers [16]. Gelatin, which is essentially denatured collagen, has a myriad of applications in the food, pharmaceutical, and cosmetic industries [17]. As for the genipin, it is a naturally occurring and low-cytotoxic crossing agent, which can be obtained from its parent compound geniposide isolated from the fruits of *Gardenia jasminoides* Ellis [18].

Neurochemical measurements of specific proteins such as neurotypic and glialtypic proteins have been used to detect injury in the developing nervous system *in vivo* [19]. Although not widely applied to date, the use of neurochemical measures of nerve regeneration has the potential to add to data obtained from the use of the aforementioned morphological measures. A number of neurotypic and glialtypic proteins have been associated with PC12 cell differentiation and Schwann cell proliferation, including growth associated protein 43 (GAP-43), presynaptic

membrane-associated proteins, such as synapsin, and type β transforming growth factors (TGF-βs) [20].

The present study examined the use of proteins associated with neurite outgrowth, synapse formation, and Schwann cell proliferation and myelination as surrogate measures of rat peripheral nerve regeneration in SRCs, genipin-crosslinked gelatin conduits (GGCs), and porous GGCs (PGGCs). This work tested the hypothesis that GAP-43, synapsin I, and TGF-β are sensitive to chemical disruption of regenerated nerves in the three types of bridging conduits. The expression of GAP-43, synapsin I, and TGF-β were determined at the same period of time and compared with axonal growth in the regenerated nerves assessed using the morphological and electrophysiological methods.

2. Materials and Methods

2.1. Manufacturing of PGGCs and GGCs

PGGCs and GGCs were constructed as described previously [21,22]. A polypropylene tubing (4.3 mm ID) was used as a mold to control the exterior shape of the PGGC. First, using a syringe, 50 ml of a 10% (w/w) solution of gelatin (300 bloom number, Sigma #G2500) in distilled water with a fine powder of gelatin was injected into the polypropylene tubing. One end of the polypropylene tubing was then

blocked with a plug. A glass rod (1.6 mm OD), used as a mandrel, was vertically pushed along the wall of the polypropylene tubing through the opening without the plug and into the gelatin paste. The open end of the polypropylene tubing was then sealed with another plug. Next, lyophilization was performed for 3 days and the specimens were retrieved from the polypropylene tubing, immersed in 0.5% (w/w) solution of genipin (Challenge Bioproducts Co., Taichung, Taiwan) for 48 h for cross-linking. The PGGC was then manually de-molded from the glass mandrel. To clean the residual genipin, the PGGCs were immersed in distilled water for 30 min, washed with distilled water for 10 times, and freeze-dried again before storage. To allow fixation of the nerve tissue to the conduit, two small holes were drilled at both ends of the PGGCs. Finally, the PGGCs were sterilized with 25 kGy of γ-ray for subsequent implantation. As for the GGCs, a 10% (w/w) solution of gelatin in distilled water at 60°C was prepared by magnetic stirring. A silicone rubber tube (1.96 mm OD; Helix Medical, Inc., Carpinteria, CA) was used as a mandrel vertically dipped into the gelatin solution. The mandrel was then withdrawn slowly and allowed to stand for 30 min for air-drying. Eight coating steps were used to obtain a gelatin tube. The gelatin-coated mandrels were then cross-linked in a 0.5% (w/w) solution of genipin for 48 h. The GGCs were then de-molded, cleaned, air-dried, and sterilized using the aforementioned methods for PGGCs.

2.2. Cross-linking degree of PGGCs and GGCs

Ninhydrin assay was used to evaluate the cross-linking degree of PGGCs and GGCs. Ninhydrin (2,2-dihydroxy-1,3-indanedione) was used to determine the amount of amino groups of each test sample. The test PGGCs and GGCs were heated with a ninhydrin solution for 20 min. After being heated with ninhydrin, the optical absorbance of the solution was recorded using a spectrophotometer (Model Genesys™ 10, Spectronic Unicam, New York, NY) at 570 nm (wavelength of the blue-purple color) using gelatin at various known concentrations as standard. The amount of free amino groups in the residual gelatin, after heating with ninhydrin, is proportional to the optical absorbance of the solution. The cross-linking degree of PGGCs and GGCs was then determined.

2.3. Bridging conduit implantation

A total of 36 adult Sprague-Dawley rats underwent placement of SRCs (1.47 mm ID, 1.96 mm OD; Helix Medical, Inc., Carpinteria, CA), GGCs, and PGGCs (12 rats per each tube group), which were removed upon sacrifice at 8 weeks. The animals were anesthetized with an inhalational anesthetic technique (AErrane®, Baxter, USA). Following the skin incision, fascia and muscle groups were separated using blunt

dissection, and the right sciatic nerve was severed into proximal and distal segments. The proximal stump was then secured with a single 9-0 nylon suture through the epineurium and the outer wall of the nerve conduits. The distal stump was secured similarly into the other end of the chamber. Both the proximal and distal stumps were secured to a depth of 2.5 mm into the chamber, leaving a 10-mm gap between the stumps. The muscle layer was re-approximated with 4-0 chromic gut sutures, and the skin was closed with 2-0 silk sutures. All animals were housed in temperature (22°C) and humidity (45%) controlled rooms with 12-hour light cycles, and they had access to food and water *ad libitum*. All animals were maintained in facilities approved by China Medical University for Accreditation of Laboratory Animal Care, and according to the regulations and standards of the National Science Council of Health of the Republic of China.

2.4. Electrophysiological techniques

After 8 weeks of regeneration, all the animals with apparent nerve regeneration were re-anaesthetized and the sciatic nerve exposed. The stimulating cathode was a stainless-steel monopolar needle, which was placed directly on the sciatic nerve trunk, 5-mm proximal to the transection site. The anode was another stainless-steel monopolar needle placed 3-mm proximally to the cathode. Amplitude and nerve

conductive velocity (NCV) of the evoked muscle action potentials (MAP) were recorded from gastrocnemius muscles with micro-needle electrodes linked to a computer system (Biopac Systems, Inc., USA). The amplitude and the area under the MAP curve from the baseline to the maximal negative peak were calculated. The MAP was used to calculate the NCV, which was carried out by placing the recording electrodes in the gastrocnemius muscles and stimulating the sciatic nerve proximally and distally to the bridging conduit. The NCV was then calculated by dividing the distance between the stimulating sites by the difference in latency time.

2.5. Histological measures

Immediately after the recording of muscle action potential, sciatic nerve sections were extracted from the middle of the regenerated nerve in the chamber. The rest of the nerve tissues were used for later neurochemical measurements. Following fixation, the nerve tissue was post-fixed in 0.5% osmium tetroxide, dehydrated, and embedded in Spurr's resin. The tissue was then cut to a thickness of 5 μm using a microtome (Leica EM UC6, Leica Biosystems, Mount Waverley, Australia) with a dry glass knife, stained with Toluidine Blue. All tissue samples were observed under a light microscope (Olympus IX70, Olympus Optical Co., Ltd., Japan). An image analyzer system (Image-Pro Lite, Media Cybernetics, USA), coupled to the microscope then

counted the blood vessels and calculated the cross-sectional area of each nerve section at magnifications between 40x and 400x. At least 30 to 50% of the nerve section area was randomly selected from each nerve specimen at a magnification of 400x to count the axons. The axon counts were extrapolated by using the area algorithm to estimate the total number of axons in each nerve. Axon density was then obtained by dividing the axon counts by the total nerve areas. All data are expressed as mean ± standard deviation. Statistical comparisons between groups were made using the one-way ANOVA. A p value of < 0.05 was considered statistically significant.

2.6. Neurochemical measures

GAP-43, synapsin I, and TGF-β were quantified using electrophoresis and Western blot analysis. Protein concentration of sciatic nerve extracts was determined by the Bradford method (Bio-Rad Protein Assay, Hercules, CA). Protein samples (50 μg/lane) were separated on a 10% SDS polyacrylamide gel electrophoresis (SDS-PAGE) with a constant voltage of 75 V. Electrophoresed proteins were transferred to polyvinylidene difluoride (PVDF) membrane (Millipore, Bedford, MA, 0.45 μm pore size) with a transfer apparatus (Bio-Rad Protein Assay, Hercules, CA). PVDF membranes were incubated in 5% milk in TBS buffer. Primary antibodies including GAP-43 (Abcam, Cambridge, MA), synapsin I (Millipore, Bedford, MA), and TGF-β (Millipore, Bedford, MA) and α-tubulin (Neo Markers, Fremont, CA) were diluted to 1:500 in antibody binding buffer overnight at 4°C. The immunoblots were washed three times in TBS buffer for 10 min and then immersed in the second

antibody solution containing goat anti-mouse IgG-HRP, goat anti-rabbit IgG-HRP, or donkey anti goat IgG-HRP for 1 hour and diluted 500-fold in TBS buffer. The immunoblots were then washed in TBS buffer for 10 min three times. For repeated blotting, nitrocellulose membranes were stripped with Restore Western blot stripping buffer (Pierce Biotechnology, Rockford, IL) at room temperature for 30 min. The immunoblotted proteins were visualized using an enhanced chemiluminescence ECL Western blotting luminal reagent (Santa Cruz, CA) and quantified using a Fujifilm LAS-3000 chemiluminescence detection system (Tokyo, Japan). All data are expressed as mean ± standard deviation. Statistical comparisons of Western blot data between groups were made using the one-way ANOVA. A p value of < 0.05 was considered statistically significant.

3. Results

3.1. Macroscopic observation of bridging conduits

The SRCs had a semitransparent chamber lumen (Fig. 1a) whereas the GGCs (Fig. 1b) and the PGGCs (Fig. 1c) were dark blue in appearance caused by the reaction between genipin and amino acids or proteins. The GGCs were concentric and round with rough outer surface and the inner lumen was smooth. By comparison, the PGGCs featured an outer surface with pores of variable size homogeneously traversing their wall and a partially fenestrated inner surface connected by an open trabecular meshwork.

3.2. Physical characteristics of PGGCs and GGCs

The cross-linking index of PGGCs and GGCs, expressed as a percentage of free amino groups lost during cross-linking, was 36±3%. It means that 1.0 wt.% genipin was sufficient to cross-link about 36% of the amino groups.

3.3. Macroscopic observation of nerve regenerates

After 8 weeks of implantation, all the SRCs were intact with no swelling or deformation. Brownish fibrous tissue encapsulation covered all over the chamber and the parts of the nerve stumps in the chamber openings. However, the regenerated nerve could be seen through the chamber lumen after trimming the fibrous tissue (Figs. 2a, 2b). No nerve dislocation was noted and the regenerated nerve, which was surrounded by fluid, occupied a central location within the chamber. By comparison, the GGCs featured a partially fenestrated outer layer, however, they still remained circular with a round lumen (Figs. 2c, 2d). As for the PGGCs, their process of swelling and degradation was dramatic (Figs. 2e, 2f). Only a small amount of wall residues was seen surrounding the regenerating nerve.

3.4. Morphological evaluation of regenerated nerves

The epineurial and perineurial regions of the regenerated nerves in the SRCs

consisted mainly of a collagenous connective tissue matrix in which circumferential cells resembling perineurial cells and fibroblasts were seen (Fig. 3a). The endourium components included fibroblasts, an occasional macrophage, and collagenous and, mainly, reticular fibers which surrounded Schwann cells ensheathing the axons. The nerve fibers were packed in the nerve bundles with oval appearances. Nuclei of Schwann cells were interspersed among these nerve fibers. Axons in the endoneurium were easily defined by their surrounding myelin sheaths stained dark blue by the toluidine blue (Fig. 3b). Blood vessels were numerous in the epineurium as well as in the endoneurial areas of the nerve. By comparison, the regenerated nerves in the GGCs displayed a structure with a thin epineurium surrounding by thick fibrous tissues (Fig. 3c). The endoneurium was cellular and vascularized in which thinly myelinated fibers grouped in regenerative clusters were evident. In addition, Schwann cells organized in clusters surrounding groups of unmyelinated axons were present (Fig. 3d). These axon-Schwann cluster formations, termed as regeneration units, are common organization structures seen under nerve cuff bridging conditions. As seen in the GGCs, it is still difficult to discriminate between the epineurium from the surrounding thick fibrous tissues of the regenerates in the PGGCs (Fig. 3e). However, the regenerated nerves in the PGGCs were relatively more mature compared to those in the GGCs, displaying a cellular and vascularized endoneurium in which numerous

myelinated axons had been seen (Fig. 3f).

3.5. Morphometric and electrophysiological measurements of regenerated nerves

Morphometric studies revealed constant data in regenerated nerves in the three types of bridging conduits for their mean values of myelinated axon number, axon density, and endoneurial nerve area. Specifically, the differences of the axon number (Fig. 4a) and the axon density (Fig. 4b) in the GGCs compared to the SRCs and the PGGCs reached the significant level at $p = 0.05$. In addition, the nerve regenerates in the GGCs had a significantly smaller endoneurial area compared to those in the SRCs (Fig. 4c). With respect to electrophysiology, morphometric observations were not correlated with electromyography in the regenerated nerves (Figs. 5a-5c). Only the nerves in the PGGCs had a significantly larger NCV compared to those in the SRCs and GGCs ($p < 0.05$).

3.6. Neurochemical measurements of regenerated nerves

In the Western blot analysis, the nerve regenerates in the SRCs ($p < 0.001$) and the PGGCs ($p < 0.001$) had a significantly higher expression of GAP-43 compared to those in the GGCs (Fig. 6a). In addition, the nerve regenerates in the PGGCs ($p = 0.001$) and the GGCs ($p < 0.001$) had a significantly lower expression of synapsin I

compared to those in the SRCs (Fig. 6b). On the contrary, the TGF-β expression was significantly higher in the groups of PGGC ($p < 0.001$) and GGC ($p < 0.001$) as compared to the SRC group (Fig. 6c).

4. Discussion

While designing polymer chambers used for nerve regeneration, investigators must evaluate the effect of tube characteristics on the quality of regenerated nerves. Nondegradable tubes can provide an isolated and stable environment for the nerves to regenerate across the gap and toward the distal stump. However, they may also block the nutrient and metabolic exchange between the lumen and the outside environment. To improve this disadvantage, investigators have developed biodegradable conduits which could maintain their structure integrity, permitting cell infiltration and subsequent tissue ingrowth during the regenerative processes [23,24]. In the present study, we used nondegradable SRCs and degradable GGCs and PGGCs to repair dissected rat peripheral nerve. The dynamic nature of the developing nervous system is so complex that it is not easy to assess nerve recovery in the animal just based on a single criterion. Therefore, my group tried to use electrophysiological methods accompanied with morphological observations to evaluate regenerated rat sciatic nerves in our past studies. As a result, we found large variations in the

electrophysiological measurements as seen in the present study, which may result from serious gastrocnemius muscle atrophy even though the muscle fibers had been reinnervated [25]. Gait analysis is another popular way to evaluate the nerve regenerates. However, the missing toes caused by automutilation due to nerve injury could result in inconsistent walking patterns [26]. We therefore developed the neurochemical ways in this study to assist in the morphometric measurements.

In the neurochemical analyses, the expression of GAP-43, synapsin I, and TGF-β was determined over the same time period of nerve regeneration in the bridging conduits. GAP-43 is a marker for growth cones and elongating axon of developing neurons [27]. High levels of GAP-43 expression are correlated with the beginning of neurite outgrowth. As for the synapsins, they are abundant phosphoproteins essential for regulating neurotransmitter release and increase in level with the formation of mature synapses in developing cell cultures [28]. In the present study, the expression of GAP-43 and synapsin I of nerve regenerates was significantly higher in the group of SRCs as compared to the GGCs. This result is similar to the morphological measurements of nerve regeneration in that the regenerates in the GGCs had a less mature microstructure with a significantly smaller area containing fewer myelinated axons. These results imply that though the SRCs were nondegradable, they still presented a good framework for the nerve fibers to regenerate across the gap and

toward the distal stump. On the contrary, the GGCs had fewer myelinated axons with numerous degenerating fibers even after 8 weeks of regeneration, though these bridging conduits were degradable. Interestingly, regenerates in PGGCs had more myelinated axons as compared to those in GGCs. Accordingly, these results indicate that how to select a suitable material used for nerve entubulization is a serious challenge. We believe that the nondegradable material, such as the silicone rubber used in this study, is the best candidate in constructing the bridging conduit for its superior properties which can provide a continuous and stable growth environment for the regenerating nerves. By comparison, a delay in temporal events of nerve regeneration was noted in the GGCs compared to those in the SRCs. It is most likely that the GGCs degraded at a rate slower than expected, resulting in their degraded materials and the metabolites produced by the regenerating nerves were sealed up in the tube lumens. This could trigger the cellular activity vigorously, causing deleterious effects on the regenerating nerves. The controversial result was dramatically improved by using the PGGCs, suggesting that the progressive increase in wall permeability of bridging conduits could accelerate collapse of the tube walls, allowing evacuation for the hazardous materials and entrance of more nutrients and cells that could promote nerve regeneration.

As for the TGF-β, it is a potent mitogen for purified rat Schwann cells which

can stimulate DNA synthesis in quiescent cells and increase their proliferation rate [29]. In adult animals, Schwann cells can provide their basal lamina as a substratum for the regenerating axons to adhere and grow [30]. In the present study, the expression of TGF-β of nerve regenerates was significantly higher in the groups of GGCs and PGGCs as compared to the SRCs. This result is not consistent with our morphometric measurements since if the Schwann cells are beneficial to regenerating axons, the expression of TGF-β of nerve regenerates in the SRCs should be higher than that in the GGCs. This result inspired us to look deeper into the TGF-β for its role playing in the nerve regeneration. In the literature, we found that the TGF-β had versatile functions. In addition to the Schwann cell proliferation-promoting capability, the TGF-β can also activate monocytes, generating fibroblast growth-promoting factors to induce fibrosis [31]. Based on these theories, we believe the high levels of TGF-β in the PGGCs and GGCs were coming from the thick fibrous tissues at the outer layers of the nerve regenerates. By comparison, the nerve regenerates in the SRCs had no such mass with only a thin epineurium surrounding the inner endoneurium.

5. Conclusions

In conclusion, our data suggest that measurements of protein associated with

axonal outgrowth and neuronal maturation have the potential to serve as surrogate markers of peripheral nerve regeneration. In particular, changes in GAP-43 and synapsin I expression correlated well with axon growth in bridging conduits made by different types of biomaterials. For TGF-β, its versatile biochemical functions may deviate histological observations from morphological measures of the regenerated nerves.

Acknowledgements

The authors would like to thank China Medical University and Hospital (CMU96-172; CMU97-139; DMR-97-055; DMR-98-054) and Taiwan Department of Health Clinical Trial and Research Center of Excellence (Contract No. DOH100-TD-B-111-004) for financially supporting this research.

References

[1] R. Langer, "Editorial: tissue engineering: perspectives, challenges, and future directions," *Tissue Eng. Part A*, 13: 1-2, 2007.

[2] H. Hosseinkhani, M. Hosseinkhani, S. Hattori, R. Matsuoka and N. Kawaguchi, "Micro and nano-scale in vitro 3D culture system for cardiac stem cells," *J. Biomed. Mater. Res.*, 94A: 1-8, 2010.

[3] F. Tian, H. Hosseinkhani, M. Hosseinkhani, A. Khademhosseini, Y. Yokoyama, G. G. Estrada and H. Kobayashi, "Quantitative analysis of cell adhesion on aligned micro- and nanofibers," *J. Biomed. Mater. Res.*, 84A: 291-299, 2008.

[4] A. Akkouch, Z. Zhang and M. Rouabhia, "novel collagen /hydroxyapatite /poly(lactide-co-ε-caprolactone) biodegradable and bioactive 3D porous scaffold for bone regeneration," *J. Biomed. Mater. Res.*, 96A: 693-704, 2011.

[5] S. Berski, J. van Bergeijk, D. Schwarzer, Y. Stark, C. Kasper, T. Scheper, C. Grothe, R. Gerardy-Schahn, A. Kirschning and G. Dräger, "Synthesis and biological evaluation of a polysialic acid-based hydrogel as enzymatically degradable scaffold material for tissue engineering," *Biomacromolecules*, 9: 2353-2359, 2008.

[6] V. T. Ribeiro-Resende, B. Koenig, S. Nichterwitz, S. Oberhoffner and B. Schlosshauer, "Strategies for inducing the formation of bands of Büngner in peripheral nerve regeneration," *Biomaterials*, 30: 5251-5259, 2009.

[7] C. M. Valmikinathan, S. Defroda and X. Yu, "Polycaprolactone and bovine serum albumin based nanofibers for controlled release of nerve growth factor," *Biomacromolecules*, 10: 1084-1089, 2009.

[8] J. D. Yuan, W. B. Nie, Q. Fu, X. F. Lian, T. S. Hou and Z. Q. Tan, "Novel three-dimensional nerve tissue engineering scaffolds and its biocompatibility with

Schwann cells," *Chin. J. Traumatol.*, 12: 133-137, 2009.

[9] K. P. Das, T. M. Freudenrich and W. R. Mundy, "Assessment of PC12 cell differentiation and neurite growth: a comparison of morphological and neurochemical measures," *Neurotoxicol. Teratol.*, 26: 397-406, 2004.

[10] I. P. Clements, Y. T. Kim, A. W. English, X. Lu, A. Chung and R. V. Bellamkonda, "Thin-film enhanced nerve guidance channels for peripheral nerve repair," *Biomaterials*, 30: 3834-3846, 2009.

[11] C. M. Lu, C. J. Chang, C. M. Tang, H. C. Lin, S.C. Hsieh, B. S. Liu and W. C. Huang, "Effects of asymmetric polycaprolactone discs on co-culture nerve conduit model," *J. Med. Biol. Eng.*, 29: 76-82, 2009.

[12] H. Jiao, J. Yao, Y. Yang, X. Chen, W. Lin, Y. Li, X. Gu and X. Wang, "Chitosan/polyglycolic acid nerve grafts for axon regeneration from prolonged axotomized neurons to chronically denervated segments," *Biomaterials*, 30: 5004-5018, 2009.

[13] G. Lundborg, B. Rosén, S. O. Abrahamson, L. Dahlin and N. Danielsen, "Tubular repair of the median nerve in the human forearm. Preliminary findings," *J. Hand Surg.*, 19: 273-276, 1994.

[14] J. H. Huang, D. K. Cullen, K. D. Browne, R. Groff, J. Zhang, B. J. Pfister, E. L. Zager and D. H. Smith, "Long-term survival and integration of transplanted

engineered nervous tissue constructs promotes peripheral nerve regeneration," *Tissue Eng. Part A*, 15: 1677-1685, 2009.

[15] Y. Xiong, Y. S. Zeng, C. G. Zeng, B. L. Du, L. M. He, D. P. Quan, W. Zhang, J. M. Wang, J. L. Wu, Y. Li and J. Li, "Synaptic transmission of neural stem cells seeded in 3-dimensional PLGA scaffolds," *Biomaterials*, 30: 3711-3722, 2009.

[16] Y. S. Chen, J. Y. Chang, C. Y. Cheng, F. J. Tsai, C. H. Yao and B. S. Liu, "An in vivo evaluation of a biodegradable genipin-cross-linked gelatin peripheral nerve guide conduit material," *Biomaterials*, 26: 3911-3918, 2005.

[17] Y. S. Chen, S. M. Kuo and C. H. Yao, "A review for gelatin used for artificial nerve and bone implants- 10-year retrospection," *Biomed. Eng. Appl. Basis Comm.*, 21: 233-238, 2009.

[18] M. C. Chen, C. T. Liu, H. W. Tsai, W. Y. Lai, Y. Chang and H. W. Sung, "Mechanical properties, drug eluting characteristics and in vivo performance of a genipin-crosslinked chitosan polymeric stent," *Biomaterials*, 30: 5560-5571, 2009.

[19] H. A. El-Fawal and J. P. O'Callaghan, "Autoantibodies to neurotypic and gliotypic proteins as biomarkers of neurotoxicity: assessment of trimethyltin (TMT)," *Neurotoxicology*, 29: 109-115, 2008.

[20] A. Gal, K. Pentelenyi, V. Remenyi, E. A. Wappler, G. Safrany, J. Skopal and Z.

Nagy, “Bcl-2 or bcl-XL gene therapy increases neural plasticity proteins nestin and c-fos expression in PC12 cells,” *Neurochem. Int.*, 55: 349-353, 2009.

[21] M. C. Lu, S. W. Hsiang, T. Y. Lai, C. H. Yao, L. Y. Lin and Y. S. Chen, “Influence of cross-linking degree of a biodegradable genipin-cross-linked gelatin guide on peripheral nerve regeneration,” *J. Biomater. Sci. Polym. Ed.*, 18: 843-863, 2007.

[22] J. Y. Chang, T. Y. Ho, H. C. Lee, Y. L. Lai, M. C. Lu, C. H. Yao and Y. S. Chen, “Highly permeable genipin-cross-linked gelatin conduits enhance peripheral nerve regeneration,” *Artif. Organs*, 33: 1075-1085, 2009.

[23] Y. Z. Bian, Y. Wang, G. Aibaidoula, G. Q. Chen and Q. Wu, “Evaluation of poly(3-hydroxybutyrate-co-3-hydroxyhexanoate) conduits for peripheral nerve regeneration,” *Biomaterials*, 30: 217-225, 2009.

[24] P. Plikk, S. Målberg and A. C, ”Albertsson. Design of resorbable porous tubular copolyester scaffolds for use in nerve regeneration,” *Biomacromolecules*, 10: 1259-1264, 2009.

[25] H. T. Chen, C. H. Yao, P. D. Chao, Y. C. Hou, H. M. Chiang, C. C. Hsieh, C. J. Ke and Y. S. Chen, “Effect of serum metabolites of Pueraria lobata in rats on peripheral nerve regeneration: in vitro and in vivo studies,” *J. Biomed. Mater. Res. B Appl. Biomater.*, 84: 256-262, 2008.

[26] M. F. Meek, J. Ijkema-Paassen and A, ”Gramsbergen. Functional recovery after transection of the sciatic nerve at an early age: a pilot study in rats,” *Dev. Med. Child Neurol.*, 49:377-379, 2007.

[27] J. J. Xu, E. Y. Chen, C. L. Lu and C. He, “Recombinant ciliary neurotrophic factor promotes nerve regeneration and induces gene expression in silicon tube-bridged transected sciatic nerves in adult rats,” *J. Clin. Neurosci.*, 16: 812-817, 2009.

[28] W. L. Coleman and M. Bykhovskaia, “Synapsin I accelerates the kinetics of neurotransmitter release in mouse motor terminals,” *Synapse*, 63: 531-533, 2009.

[29] E. O. Johnson, A. Charchanti and P. N. Soucacos, “Nerve repair: experimental and clinical evaluation of neurotrophic factors in peripheral nerve regeneration,” *Injury*, 39 Suppl. 3: S37-S42, 2008.

[30] A. Pierucci, E. A. Duek and A. L. de Oliveira, “Expression of basal lamina components by Schwann cells cultured on poly(lactic acid) (PLLA) and poly(caprolactone) (PCL) membranes,” *J. Mater. Sci. Mater. Med.*, 20: 489-495, 2009.

[31] K. R. Cutroneo, “TGF-beta-induced fibrosis and SMAD signaling: oligo decoys as natural therapeutics for inhibition of tissue fibrosis and scarring,” *Wound Repair Regen.*, 15 Suppl. 1: S54-S60, 2007.

Captions

Fig. 1. Macrographs of (a) SRC, (b) GGC, and (c) PGGC.

Fig. 2. (a) SRC, (c) GGC, and (e) PGGC 8 weeks of implantation. Regenerated nerve exposed after trimming the remained bridging materials of (b) SRC, (d) GGC, and (f) PGGC.

Fig. 3. Photomicrographs of regenerated sciatic nerve sections 8 weeks after surgery stained with Toluidine Blue. (a) Regenerated nerve repaired with SRC had a well-defined structure in which the endoneurium (circle inside) was highly cellular and vascularized. In the epineurium, circumferential cells resembling perineurial cells (asterisks in insert and (a)) and fibroblasts (small arrow in insert and (a)) were seen. By comparison, regenerated nerve repaired with (c) GGC formed thick fibrous tissues and a thin epineurium (regions between arrows in insert and (c)) surrounding the inner endoneurium (circle inside). (e) Similarly, thick fibrous tissues of the regenerates were seen in the PGGCs. Abundant myelinated axons were seen in the regenerated nerves repaired with (b) SRC and (f) PGGC. (d) In the GGC, thinly myelinated fibers grouped in regenerative clusters (arrows) were evident accompanied by numerous degenerating fibers In addition, Schwann cells organized in clusters surrounding groups of unmyelinated

axons were present (arrowheads in insert and (d)). Scale bars in a, c and e = 100 μm; b, d and f = 30 μm; insert in (a), (d) = 20 μm, (c) = 30 μm.

Fig. 4. Morphometric analysis from regenerated nerves in bridging conduits, including (a) myelinated axon count, (b) axon density, and (c) endoneurial area. Data are means ± S.E. (n=12). *Significantly different at $p<0.05$.

Fig. 5: Analysis of the evoked muscle action potentials, including (a) peak amplitude, (b) MAP area, and (c) NCV. *Significantly different at $p<0.05$.

Fig. 6. Representative immunoblots for (a) GAP-43, (b) synapsin I, and (c) TGF-β, and quantification of the three protein levels in regenerated nerves. *Significantly different at $p<0.05$.

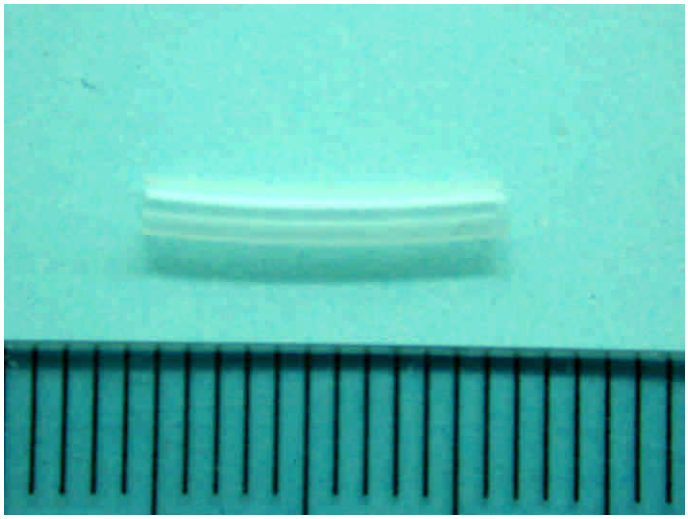

Fig. 1a

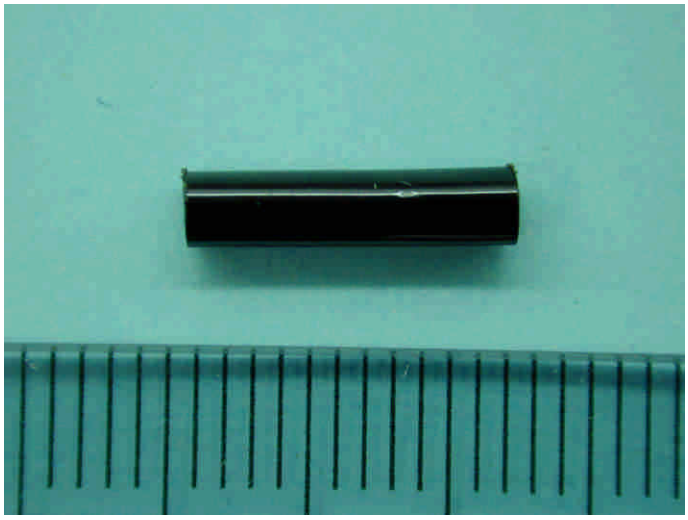

Fig. 1b

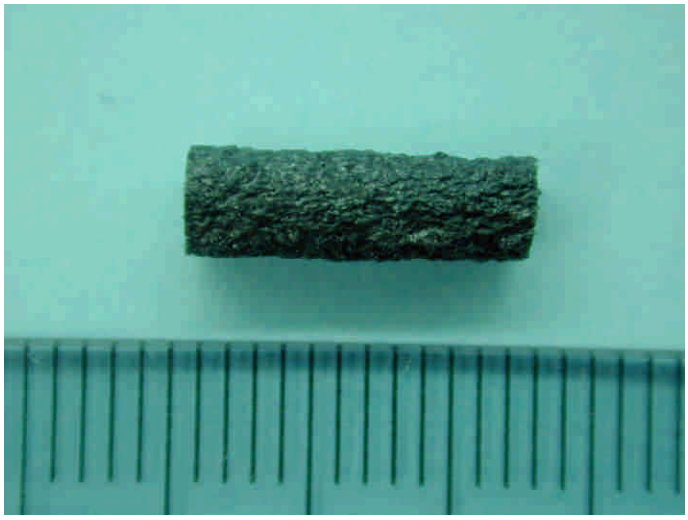

Fig. 1c

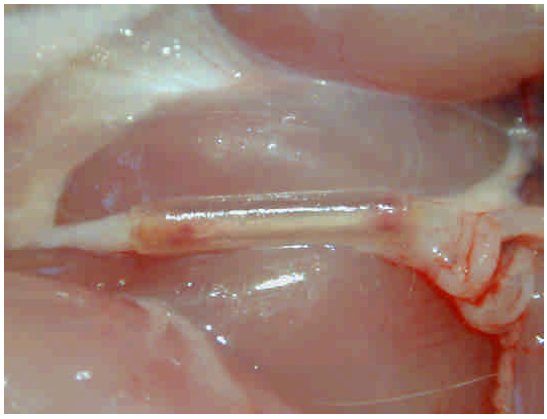

Fig. 2a

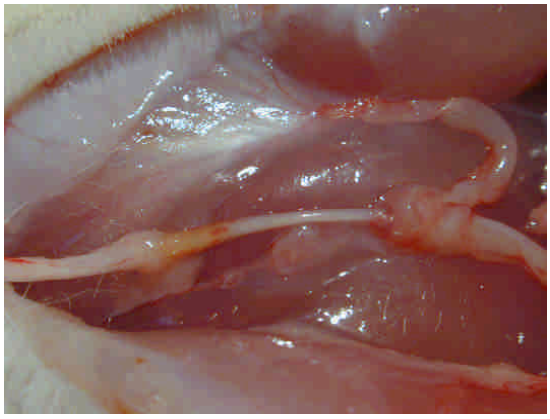

Fig. 2b

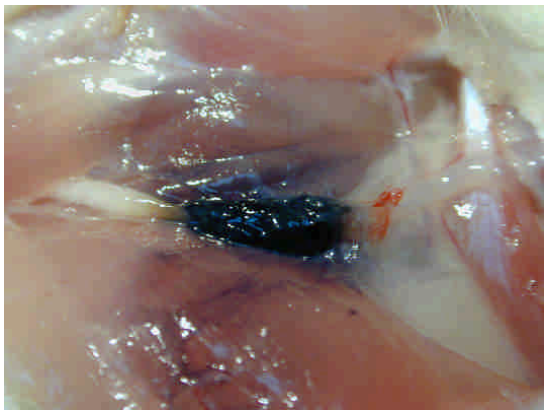

Fig. 2c

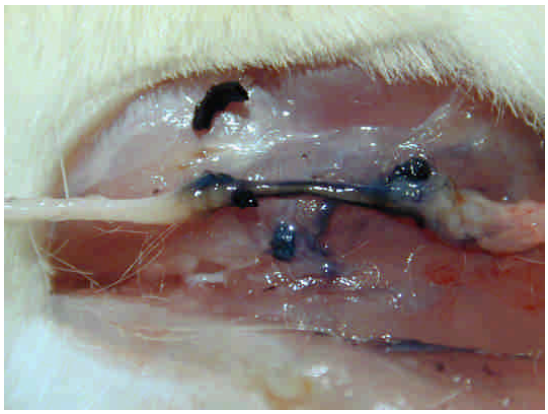

Fig. 2d

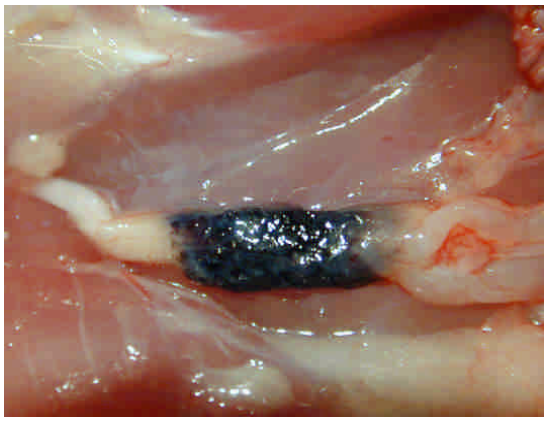

Fig. 2e

Fig. 2f

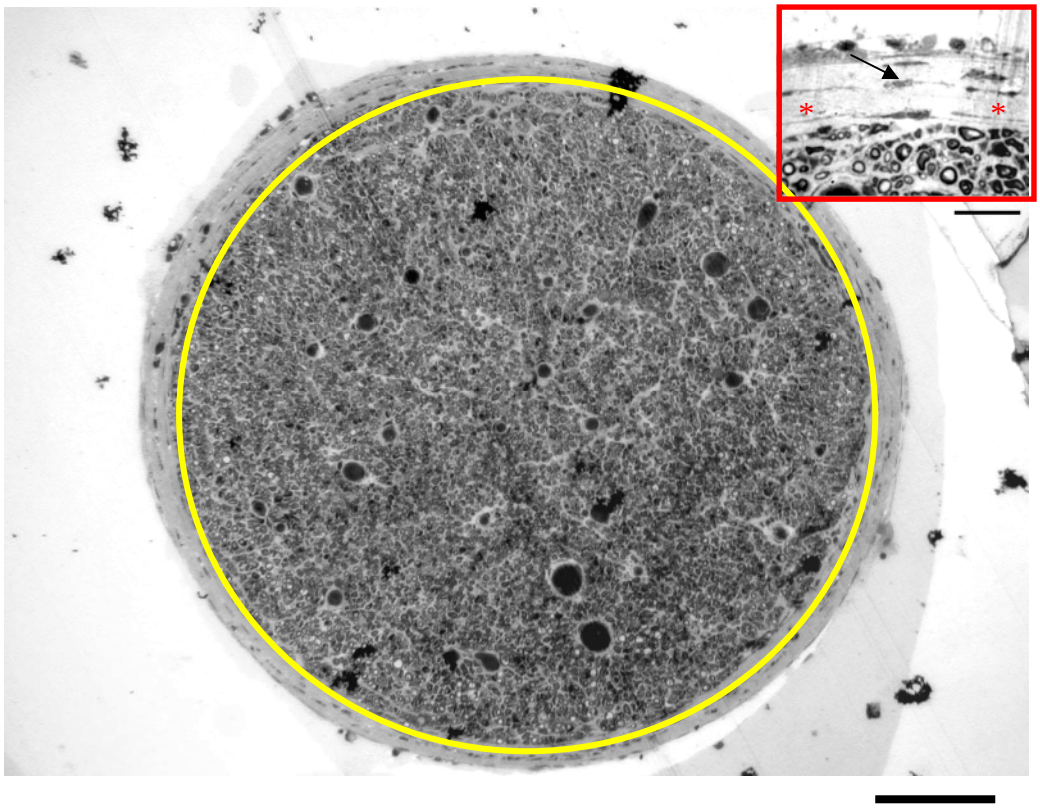

Fig. 3a

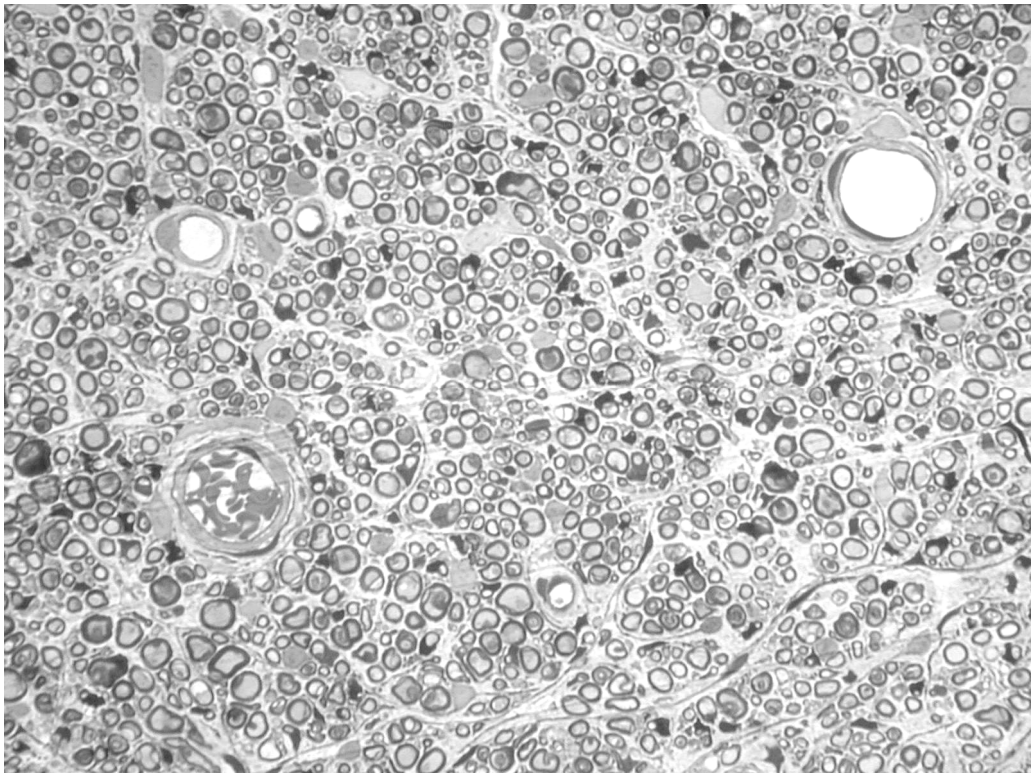

Fig. 3b

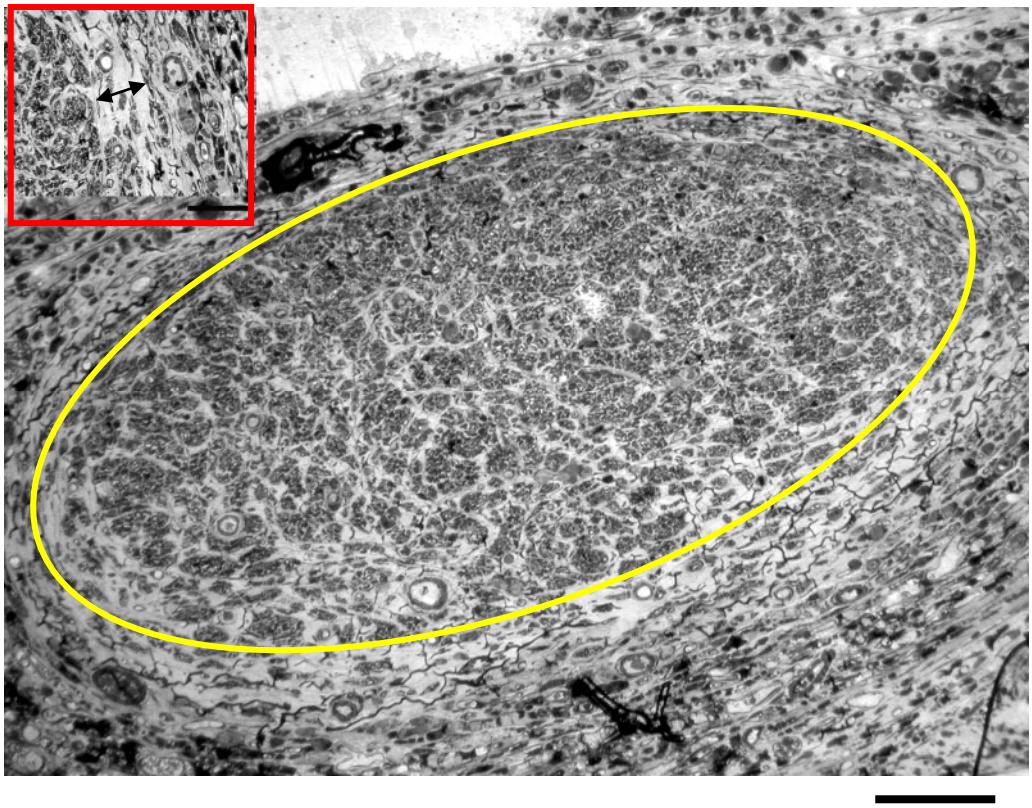

Fig. 3c

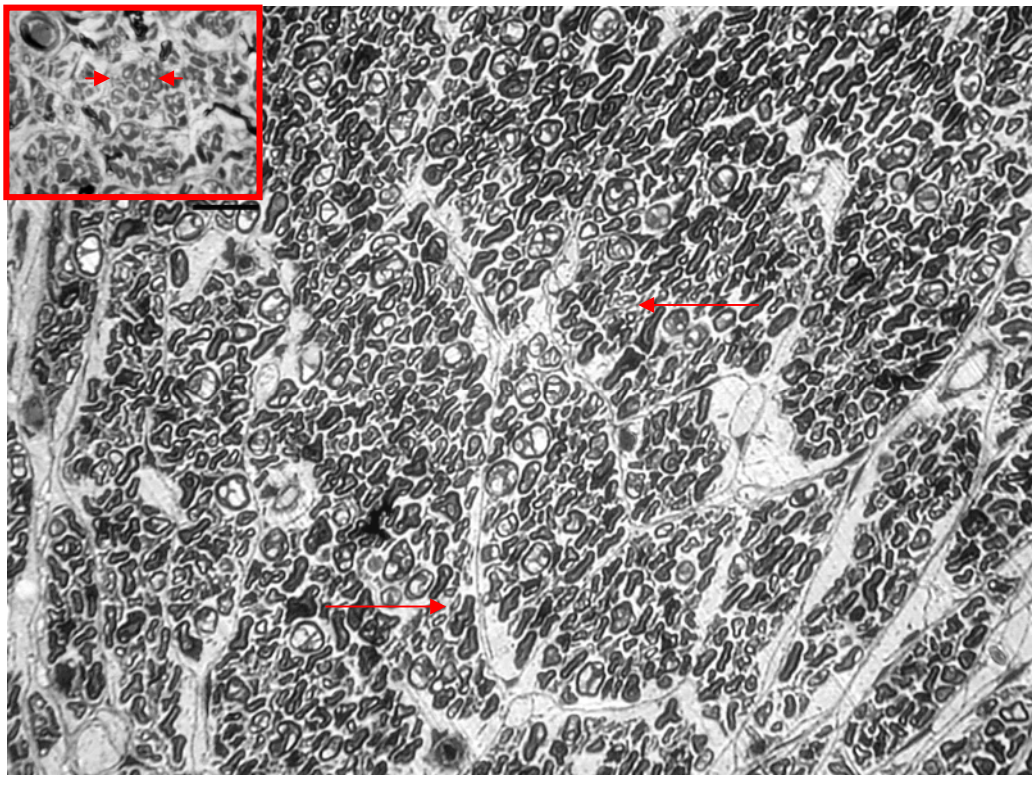

Fig. 3d

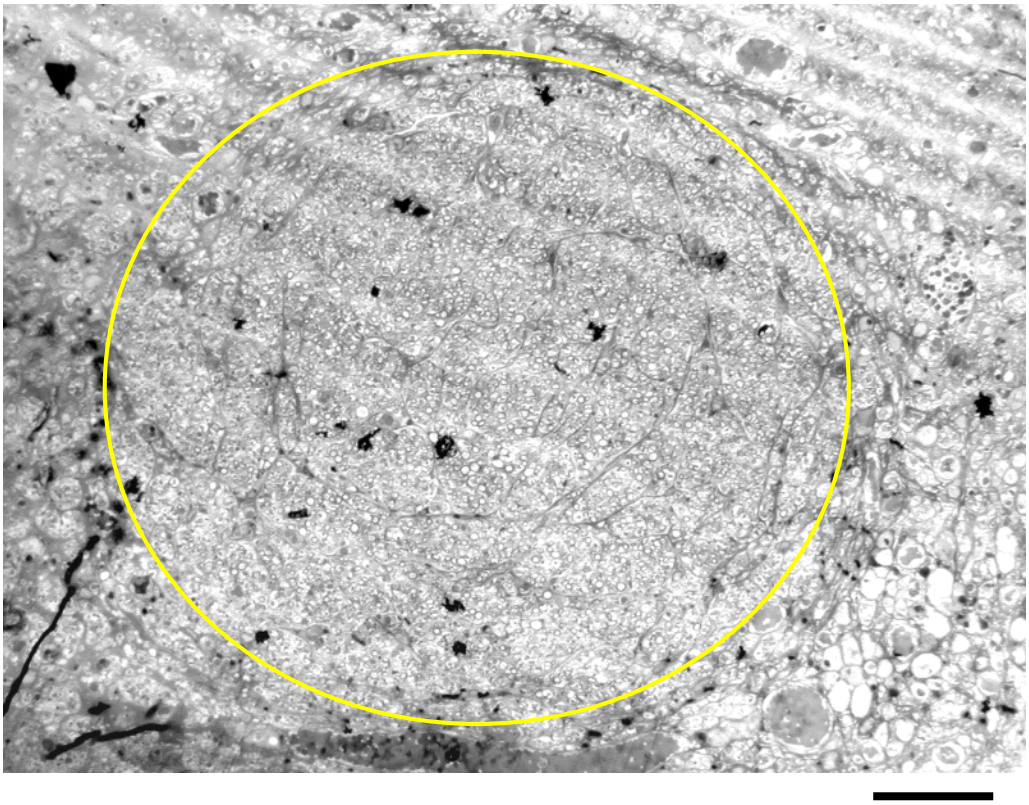

Fig. 3e

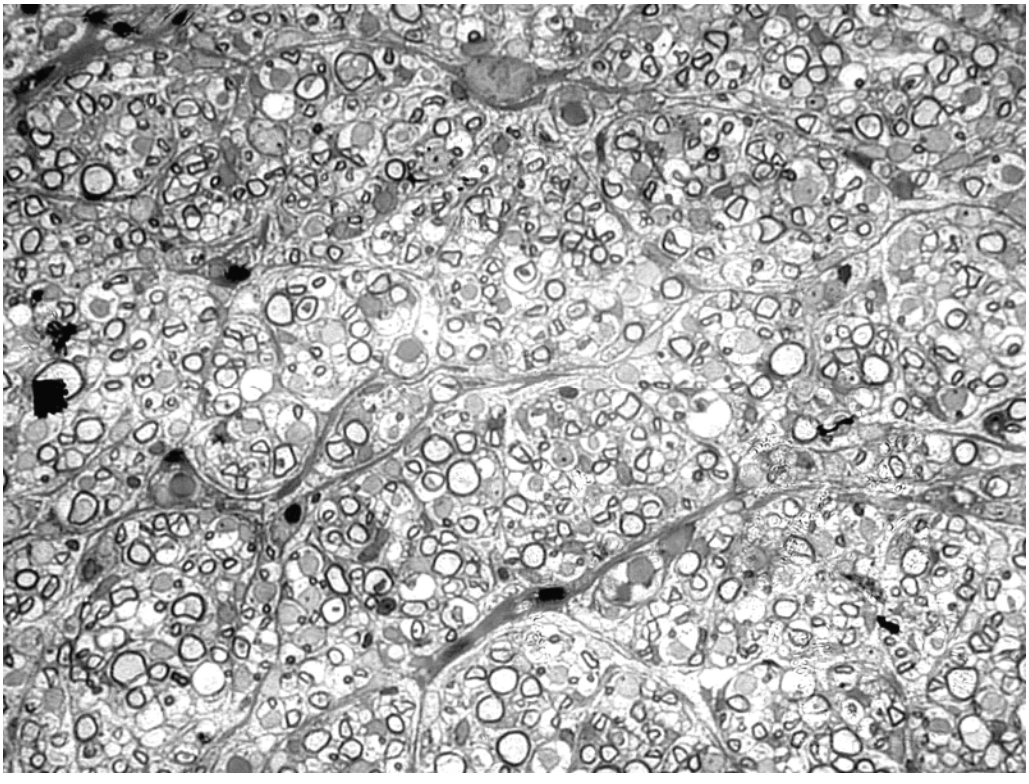

Fig. 3f

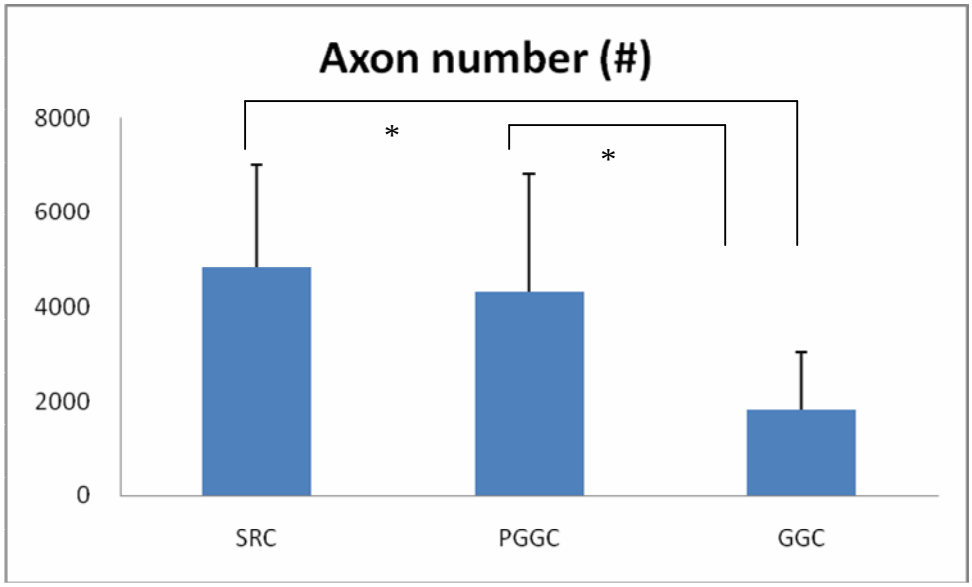
Axon number (#)
8000
6000
4000
2000
0
*
*
SRC
PGGC
GGC

Fig. 4a

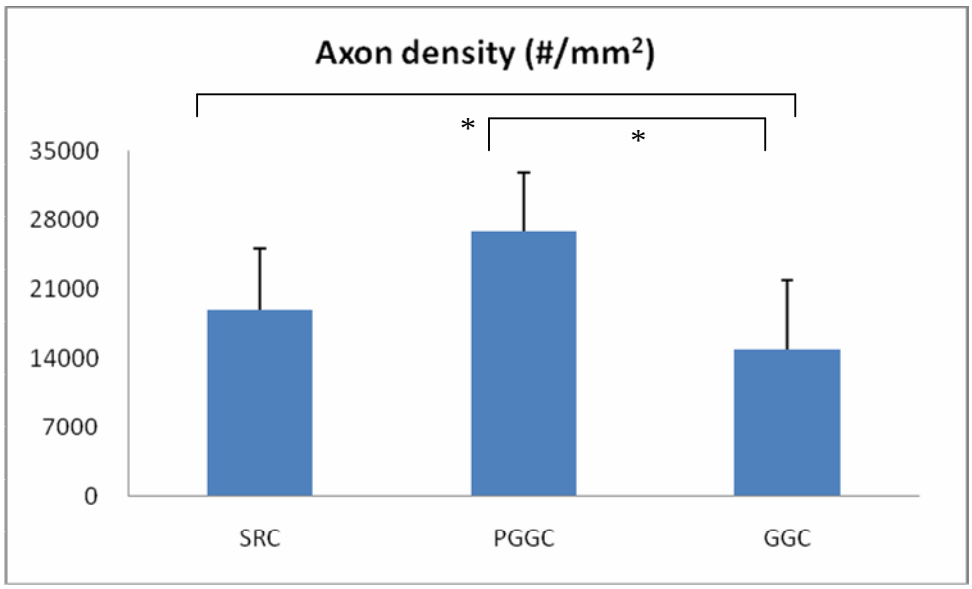
Axon density (#/mm²)
35000
28000
21000
14000
7000
0
*
*
SRC
PGGC
GGC

Fig. 4b

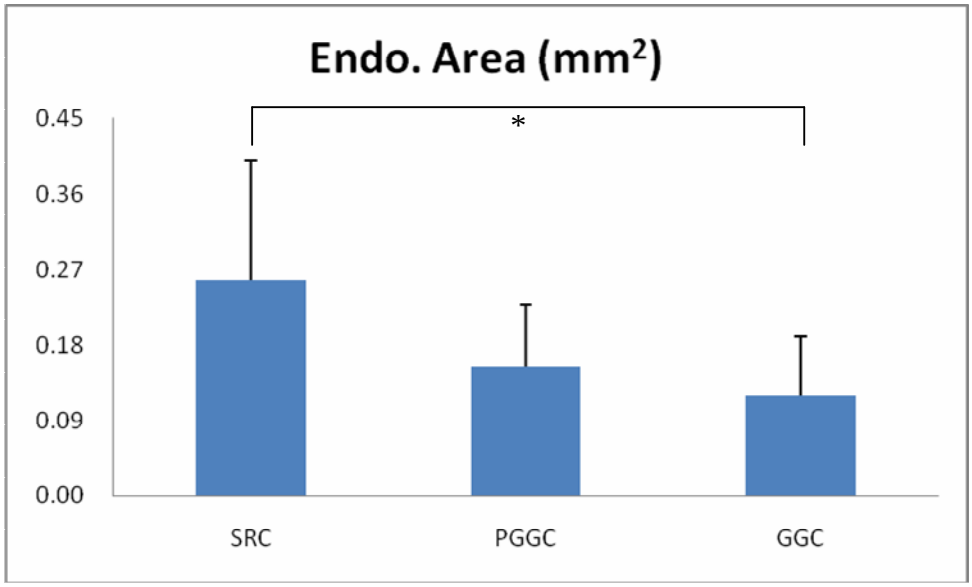

Fig. 4c

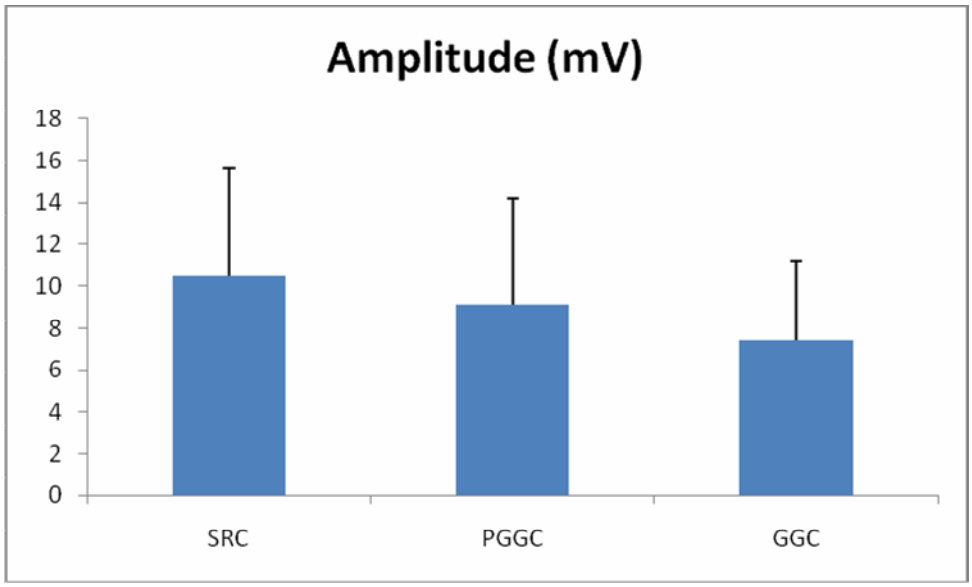
Amplitude (mV)
18
16
14
12
10
8
6
4
2
0
SRC
PGGC
GGC

Fig. 5a

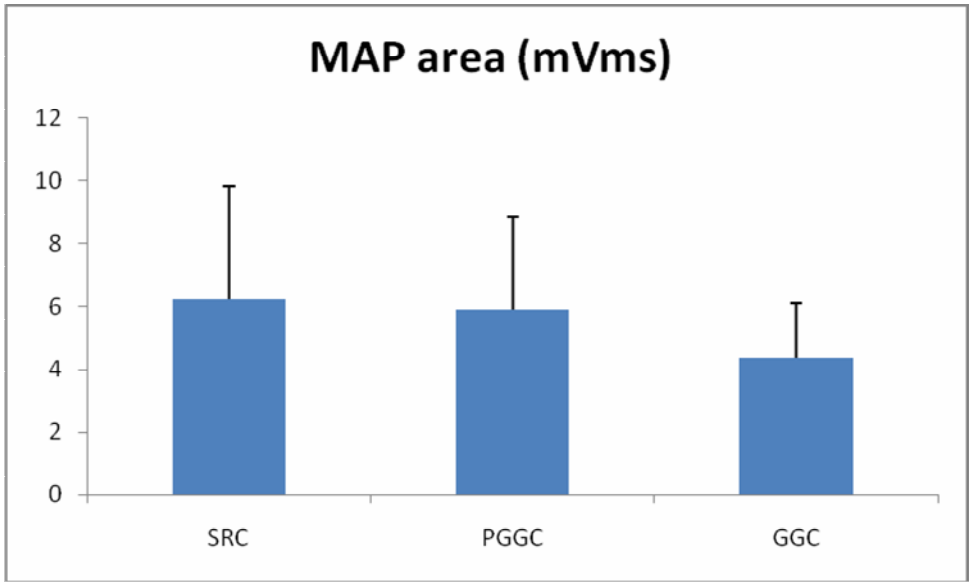
MAP area (mVms)
12
10
8
6
4
2
0
SRC
PGGC
GGC

Fig. 5b

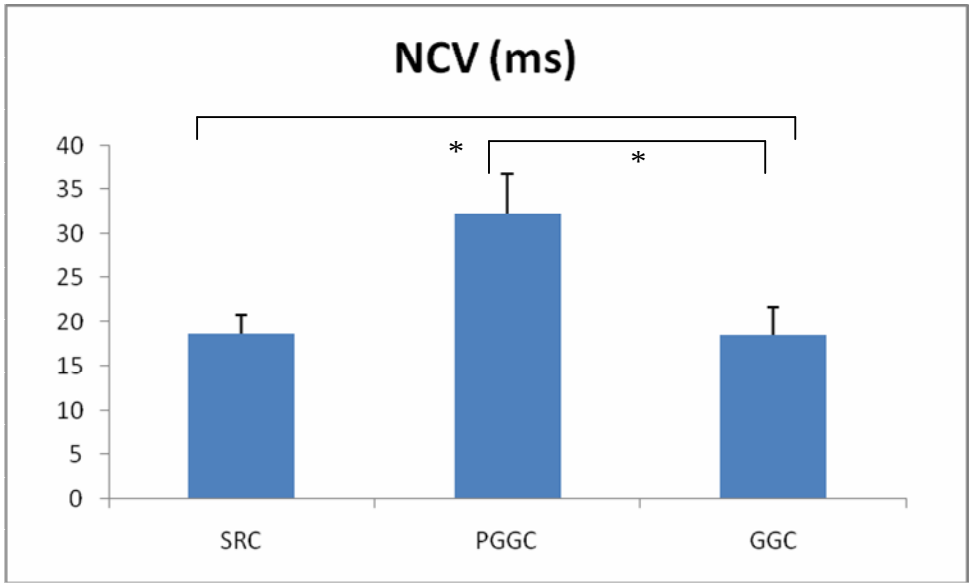

Fig. 5c

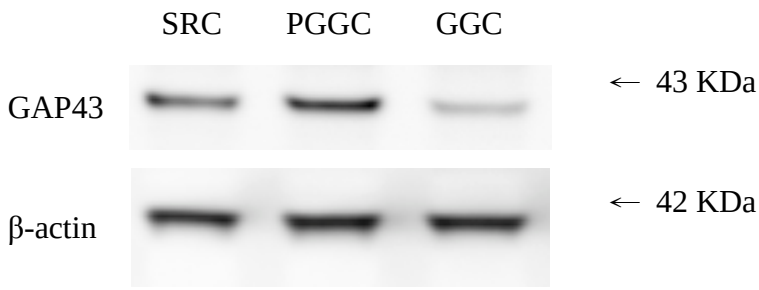
SRC
PGGC
GGC
GAP43
← 43 KDa
β-actin
← 42 KDa

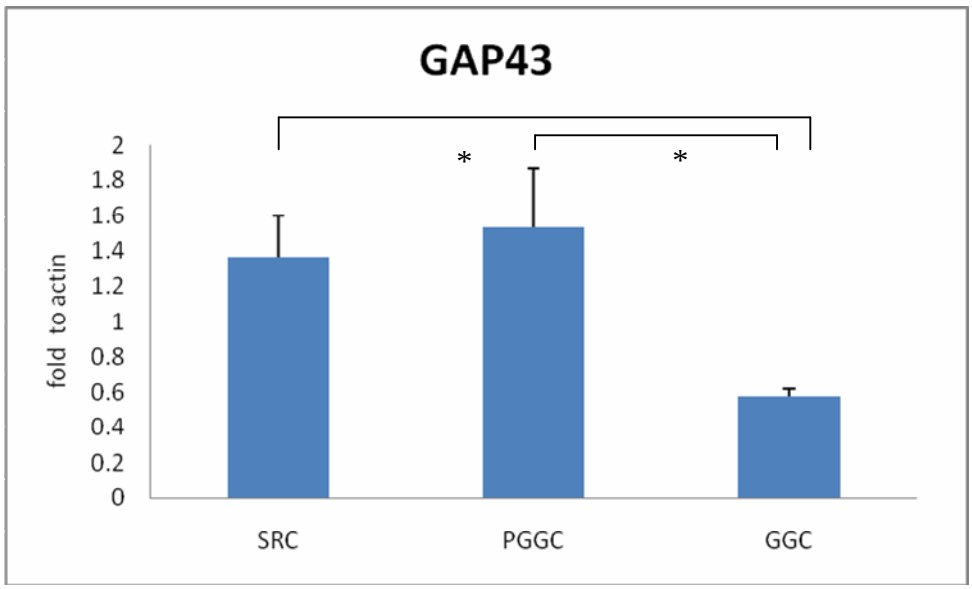
GAP43
fold to actin
2
1.8
1.6
1.4
1.2
1
0.8
0.6
0.4
0.2
0
*
*
SRC
PGGC
GGC

Fig. 6a

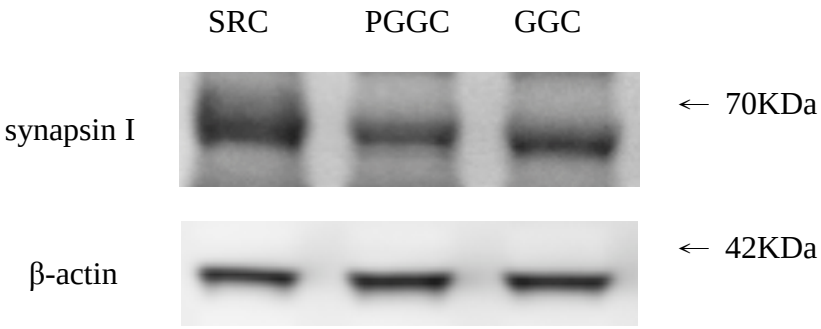
SRC
PGGC
GGC
synapsin I
← 70KDa
β-actin
← 42KDa

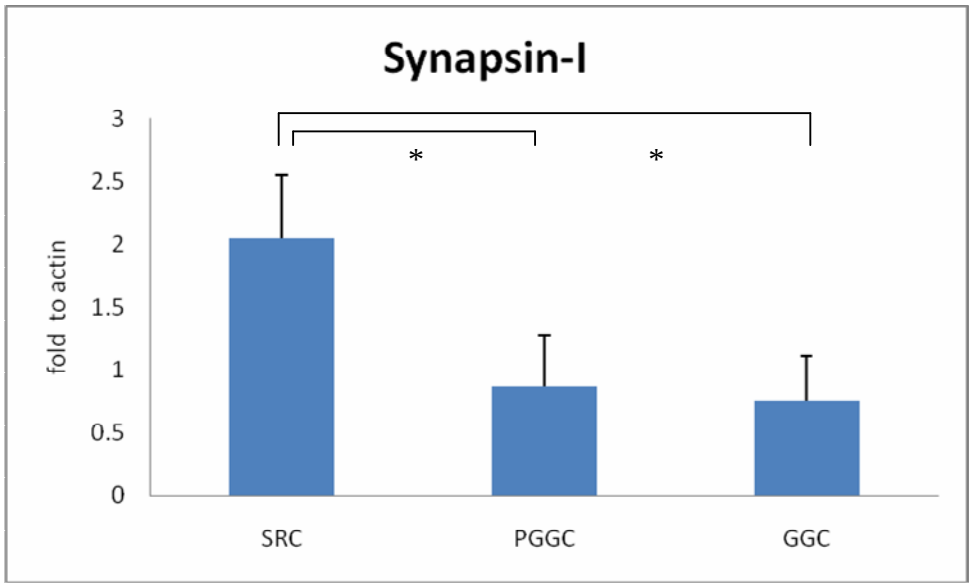
Synapsin-I
fold to actin
3
2.5
2
1.5
1
0.5
0
*
*
SRC
PGGC
GGC

Fig. 6b

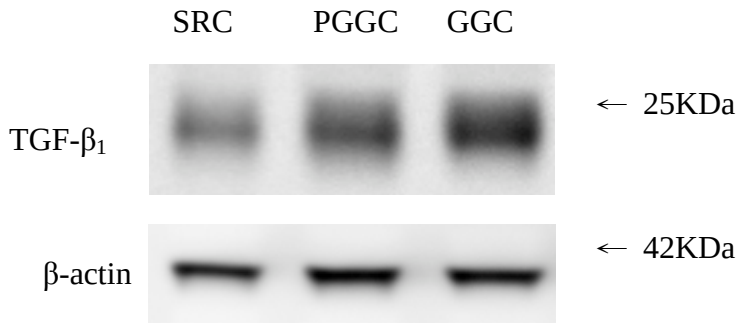
SRC
PGGC
GGC
TGF-β1
← 25KDa
β-actin
← 42KDa

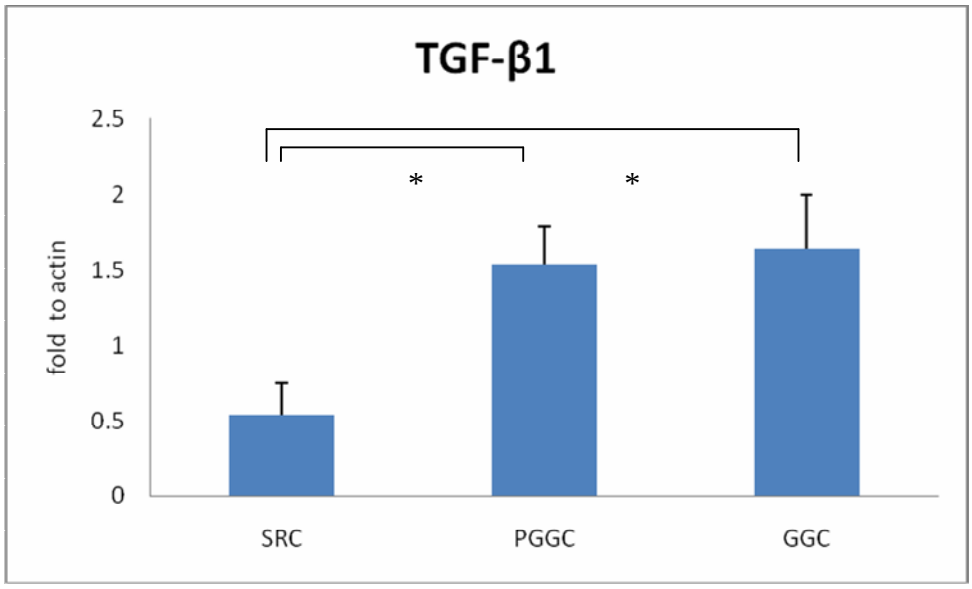
TGF-β1
fold to actin
2.5
2
1.5
1
0.5
0
*
*
SRC
PGGC
GGC

Fig. 6c